ELSEVIER

Journal of Nuclear Materials 255 (1998) 165–173

journal of nuclear materials

Identification of the nature of small point defect clusters in neutron irradiated Fe–16Ni–15Cr by means of electron irradiation

M. Horiki [a,*], S. Arai [a], Y. Satoh [b], M. Kiritani [c]

[a] *Department of Nuclear Engineering, School of Engineering, Nagoya University, Furo-cho, Chikusa-ku, Nagoya 464-01, Japan*
[b] *Research Reactor Institute, Kyoto University, Kumatori-cho, Sennan-gun, Osaka 590-04, Japan*
[c] *Department of Electronics, Hiroshima Institute of Technology, Miyake, Saiki-ku, Hiroshima 731-51, Japan*

Received 21 February 1997; accepted 29 January 1998

Abstract

The nature of very small point defect clusters in Fe–16Ni–15Cr irradiated with fission neutrons was identified from their behavior under electron irradiation with a high voltage electron microscope. In this analysis, the defect clusters which grew during electron irradiation were judged to be of interstitial (I)-type and those which shrank or disappeared to be of vacancy (V)-type. The fraction of the number of I- and V-type defect clusters in a specimen irradiated as a bulk at 353 K were found to be 7% and 93%, respectively. In a specimen irradiated at 623 K as a bulk, most of defect clusters were I-type with a very small fraction of V-type. In a thin foil specimen irradiated at 573 K, the fraction of I-type defect clusters increased from 20% near the thin specimen edge to 70% at a thicker part of 120 nm. These results were consistent with those in the previous judgement from the shape and contrast of transmission electron microscope image.

PACS: 61.16.Bq; 61.72.Ji; 61.80.Hg

1. Introduction

Austenitic stainless steels are structural materials in various types of fission neutron reactors and are one of the candidate materials for future fusion reactors.

In the previous study by the present authors [1], microstructural evolution reflecting primary damage in a Fe–16Ni–15Cr alloy (model alloy of austenitic stainless steels) irradiated by JMTR (Japan Material Testing Reactor) with an improved temperature control was examined. Interstitial (I)-type defect clusters appeared as dislocation loops at all temperatures examined (373 K–673 K). The size and the number density of I-type clusters depended strongly on the irradiation temperature with larger size and lower number density at higher temperature. Vacancy (V)-type clusters appeared as stacking fault tetrahedra (SFT) at lower temperatures and as voids at higher temperatures. By the comparison of the damage structures between specimens irradiated as thin foil and as bulk, the role of freely migrating defects was extracted.

During the course of the study, the interpretation from the experimental data was based on the nature of point defect clusters judged from the shape and contrast of images obtained by transmission electron microscope (TEM). Although the maximum care was taken in the judgement, some uncertainty could remain.

There are several other methods to identify the nature of point defect clusters. For example, inside–outside method, which is used to identify the nature of dislocation loops from the image position of dislocation [2,3], is reliable for large loops but is not applicable for very small ones (< 20 nm). Black–white contrast method [4] has the difficulty in the accurate measurement of the depth of each defect, though it is applicable for small defects. Lastly, 2 1/2D stereo method is known to lead to erroneous results [5]. An innovation has been highly desired to break through these unsatisfactory situations.

* Corresponding author. Tel.: +81-52 789 3609; fax: +81-52 789 3791.

0022-3115/98/$19.00
PII: S0022-3115(98)00033-6

Electron irradiation produces an interstitial dominant atmosphere during an early stage of irradiation simply due to higher mobility of interstitials than vacancies [6]. From the behavior of neutron irradiation induced defects under electron irradiation, one could tell the nature of point defect clusters, I- or V-type, because the former is expected to grow and the latter to shrink or disappear.

In this paper, the procedure of electron irradiation and analysis are explained first for the identification of the nature of small defect clusters in neutron irradiated Fe–16Ni–15Cr. Next the results obtained on the size and density of I- and V-type defect clusters are compared with those obtained in the previous study [1]. Then the validity and limitation of the previous method using microscope images are re-examined.

2. Point defect processes and expected behavior of neutron irradiation induced defect clusters during electron irradiation

To anticipate the behavior of neutron irradiation induced point defect clusters during electron irradiation, a brief survey of the characteristics of point defect reaction processes during electron irradiation with a high voltage electron microscope is made from long years of research experience of one of the present authors [6]. Firstly, the damage rate is much higher than neutron irradiations [7], for example, the displacement damage rate of 10^{-4}–10^{-3}/s is achieved by an electron current density of 10^{23}–10^{24} e/cm^2 s. Secondly, the irradiation is always performed on a foil specimen appropriate for TEM observation. The inevitable use of thin foils introduces two typical situations into the point defect reaction processes during irradiation; surface sink dominant case for the combination of lower defect production rate and higher temperature, and inside-reaction dominant case for the combination of higher defect production rate and lower temperature.

During an early stage of electron irradiation of fcc metals and alloys, concentrations of interstitials and vacancies increase proportionally to the irradiation time. As irradiation proceeds, interstitials which have larger mobility react mutually and form I-type defect clusters, and consequently the concentration of interstitials starts to decrease. However, when the specimen is very thin or contains high density of defect clusters, which is the case of the present experiment, interstitials are consumed at these sinks, rather than forming their clusters. Finally, the steady-state of the point defect concentration is achieved by the balance of their production and annihilation, under the equal migration efficiencies (the product of the mobility and concentration) between interstitials and vacancies.

In the present identification technique by means of electron irradiation, growth of I-type defect clusters and shrinkage or disappearance of V-type defect clusters are expected at two different irradiation stages. One is at the initial stage of irradiation before reaching the steady-state. In this stage, the migration efficiency of interstitials is larger than that of vacancies due to the larger mobility of interstitials. The other is at the steady-state period. In this stage, though interstitials and vacancies have an equal migration efficiency, I-type defect clusters as dislocation loops continue to grow by absorbing interstitials preferentially owing to the strain field around the loops [8]. In both cases, I-type clusters are expected to grow while V-type to shrink or disappear.

In spite of the principle mentioned above, unexpected reaction may occur near sinks such as surfaces, grain boundaries or dislocations, due to the prompt escape of interstitials to these sinks. In such cases, a special care is necessary for the identification of the nature of clusters near sinks.

3. Experimental procedure

3.1. Specimens neutron irradiated and examined by electron irradiation

The material examined was Fe–16Ni–15Cr alloy, that is a simple model alloy of the Japanese prime candidate alloy (JPCA) for fusion application. Samples were prepared by direct melting of the three component high purity metals, and were rolled down to foils of 0.1 mm thickness. Punched-out disc specimens of 3 mm in diameter were heat treated for 1 h at 1273 K. Two types of specimens were prepared for neutron irradiation: one is as heat treated (bulk) and the other is a thin foil specimen electropolished for electron microscope observation (thin foil). Bulk samples are thick enough for the surface effect on microstructural evolution to be neglected. Thin foil samples were prepared so as to have a tapered thickness like a sharp knife edge. At a very thin part of the foil, freely migrating interstitials, which are released from collision cascade zone, are expected to escape to surface, and the V-type clusters produced directly from cascades are expected to be preserved. At a thicker part of the thin foil specimens and in the bulk specimens, the reaction of these freely migrating interstitials play an important role in the microstructure evolution, e.g., the elimination of V-type clusters along with the formation of I-type clusters. Thus, a comparison of defect structures developed in thin foils and bulk specimens provides useful information on the role of freely migrating point defects [9].

Neutron irradiation was carried out with JMTR at the Japan Atomic Energy Research Institute at Oarai. JMTR is the materials test reactor whose thermal output is 50 MW and whose maximum neutron flux at the core position is 4×10^{18} n/m^2 s. The irradiations were performed under the improved temperature control [10]. The irradiation

temperature and the irradiation dose ranged from 353 to 673 K and 2.5 to 11×10^{23} n/m^2, respectively.

Because of limitations in the number of neutron irradiated specimens and in the availability of the high voltage electron microscope, samples were selected so that the representative microstructures may be examined. Typical temperatures adopted as a lower and a higher temperature were 353 K and 623 K, respectively. In addition, one sample, which was irradiated at 573 K as a thin foil, was examined. The temperature of 573 K is a characteristic one for the present alloy where SFT is replaced by voids.

3.2. Electron irradiation and observation

Electron irradiation for the identification was performed with H-1250ST at Nagoya University. Among a number of high voltage electron microscopes in Japan, the H-1250ST is the only one which accepts radioactive samples. The microscope was operated at 1000 kV and the irradiation intensity of $3–5 \times 10^{24}$ e/m^2 s. The irradiation intensity in the present experiment was kept relatively low, because intense irradiation brings ambiguity in the identification by introducing new defect clusters.

All the electron irradiation was performed at the temperatures of the neutron irradiation. However, in the case that neutron irradiation was carried out at the temperature where vacancies are not highly mobile, electron irradiation was performed at 573 K after an annealing at 573 K. In this case, the change of microstructures through the annealing up to 573 K was examined before the electron irradiation and the results of the annealing was incorporated in the process of the identification of defect type by the electron irradiation.

During the irradiations, in situ observation of the variation of defects was carried out in bright-field and weak-beam dark-field imaging conditions with the H-1250ST. For the detailed comparison of the microstructures before and after the electron irradiation, the observation was made with a JEM-200CX (TEM) operated at 200 kV under the same observation conditions. The bright-field observation was suitable for defect clusters such as dislocation loops with strain field and the weak-beam dark-field observation was suitable for small defect clusters such as SFT. Stereoscopic observations were essential for the detection of the microstructural variation with the depth from specimens surfaces. This technique is particularly important for the specimens irradiated with neutrons as thin foils, where microstructures have a significant depth dependence before the electron irradiation.

4. Results and discussion

4.1. Identification of defect clusters introduced by neutron irradiation of a thin foil

4.1.1. In situ observation during electron irradiation

Fig. 1 shows the change of microstructures during electron irradiation at 573 K in a comparatively thin part (< 50 nm) of a foil specimen pre-irradiated with neutrons

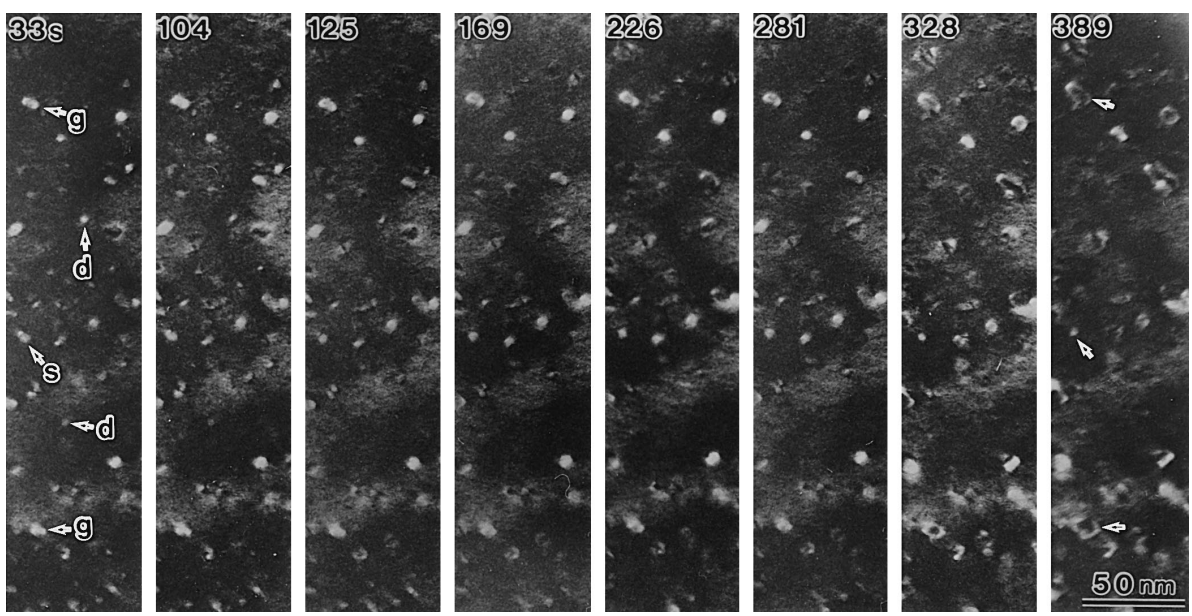

Fig. 1. Progressive change of defect structure in a thin part of Fe–16Ni–15Cr neutron irradiated thin foil (1.0×10^{24} n/m^2) at 573 K during electron irradiation at 573 K (1000 keV, 9×10^{24} e/m^2 s). Dark-field observation. Examples of the defect clusters which grew, disappeared and shrank during electron irradiation are indicated by the arrows with *g*, *d* and *s*, respectively.

at the same temperature. Microstructures before electron irradiation consist of very small defect clusters with clear contrast and those of comparatively large size with a blurred periphery.

It is clearly observed that most of defect clusters of small but clear contrast shrunk and disappeared, and larger ones with bright contrast grew. Examples of the defect clusters which grew, disappeared and shrank during electron irradiation are indicated by the arrows with *g*, *d* and *s*, respectively.

4.1.2. Influence of surface sinks on the reaction of defect clusters during electron irradiation

From the principle as described in Section 2, I-type defect clusters are expected to grow and V-type clusters to shrink or disappear by electron irradiation. However, when clusters are near sinks like the surface, abnormal reactions may occur due to prompt escape of electron-irradiation-induced interstitials to surface sinks. In this section, the relation of the reaction of defect clusters during electron irradiation to surface sinks are examined.

Fig. 2a and b show stereoscopic pair micrographs of the specimen shown in Fig. 1 before electron irradiation, and Fig. 2c the microstructure of the same area after the electron irradiation. Fig. 3 shows the spatial distribution of the change of defect clusters, shrinkage, disappearance, no change and growth by electron irradiation, and the types of clusters which were judged by our conventional judgement technique from the shape and contrast of images. In this figure, the clusters abnormally behaved, e.g., those I-type clusters which had shrank or disappeared and those V-type clusters which had grown are also indicated and they are exclusively located near the surfaces. On the other hand, at the central part of the specimen, no clusters are observed to have behaved abnormally and hence the reaction of

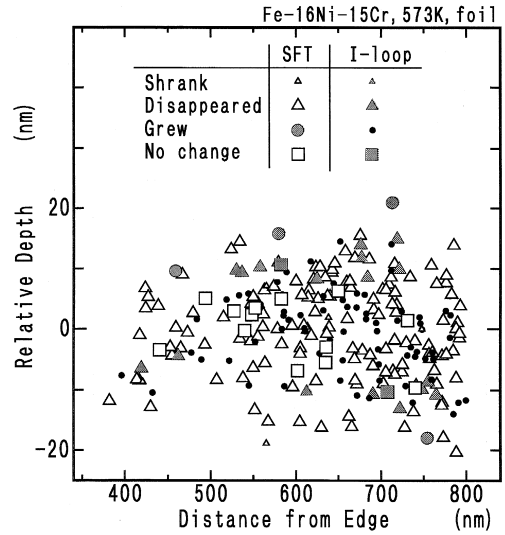

Fig. 3. Spatial distribution of the reaction of defect clusters in a thin part of the specimen during electron irradiation. In this figure, types of clusters were judged by our conventional judgement technique from the shape and contrast of images.

clusters during electron irradiation at the central part of the specimen is thought to give a confident identification of the nature. Fig. 4 shows the size distribution of the clusters at the central part which had disappeared, shrank, not changed and grown. It was found that clusters disappeared which are regarded as V-type have smaller size and clusters grown which are regarded as I-type have larger size. In this experiment, almost all the clusters smaller than 1.5 nm disappeared by electron irradiation and hence the

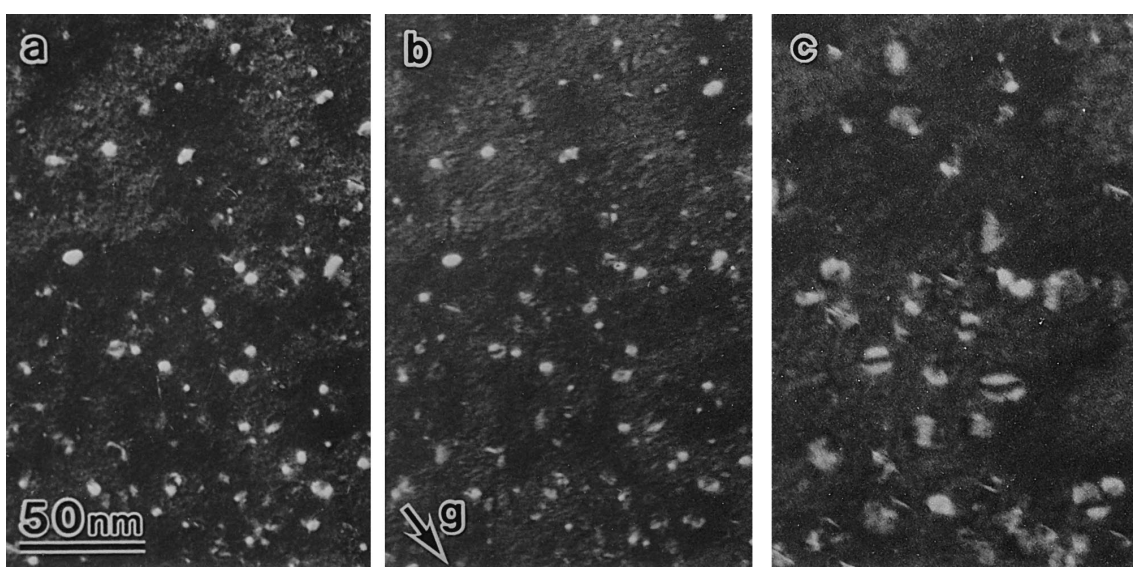

Fig. 2. (a) and (b) Stereoscopic micrograph pairs in a thin part of the specimen before electron irradiation and (c) after electron irradiation.

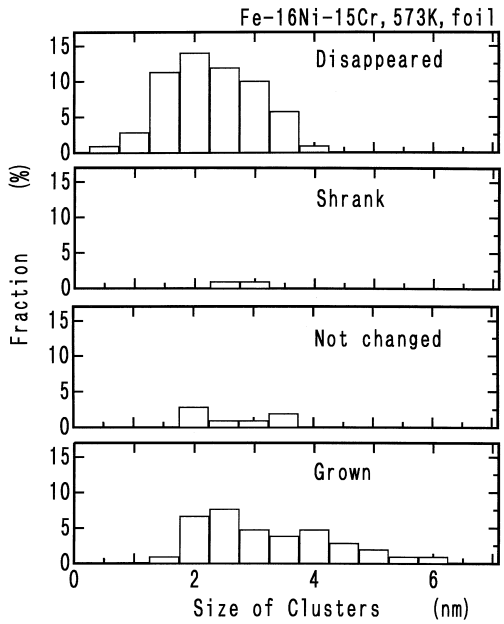

Fig. 4. Size distribution of defect clusters of four kinds of reaction at the central part of the specimen during electron irradiation.

judgement that all the clusters smaller than 1.5 nm are regarded to be of V-type will not be misleading.

The identification of the nature of clusters near surface should be done carefully in the light of the results of electron irradiation at the central part of the specimen.

4.1.3. Variation of microstructures with foil thickness

In this section, we compare the defect microstructures in a comparatively thick part with those in the thin part in a sample neutron-irradiated as a thin foil. Fig. 5 is bright-field photographs before and after electron irradiation of the thick part of the same specimen as examined in Fig. 1. As shown in Fig. 5a, faulted dislocation loops and small clusters coexist before electron irradiation. By the electron irradiation, a larger fraction of defect clusters grew compared with the case in the thinner part. Same as in Fig. 1, those clusters which have grown, disappeared and shrank are indicated by the arrows with *g*, *d* and *s*, respectively.

Fig. 6 compares the size distribution of I- and V-type defect clusters identified by electron irradiation at three different foil thickness. The number densities of I- and V-type defect clusters at each thickness were evaluated as followed: $1.1\times10^{22}/\mathrm{m}^3$ and $3.7\times10^{22}/\mathrm{m}^3$ at 20 nm, $1.6\times10^{22}/\mathrm{m}^3$ and $3.1\times10^{22}/\mathrm{m}^3$ at 40 nm, and $1.1\times10^{22}/\mathrm{m}^3$ and $3.8\times10^{21}/\mathrm{m}^3$ at 120 nm. With the increase of the foil thickness, the fraction of V-type defect clusters

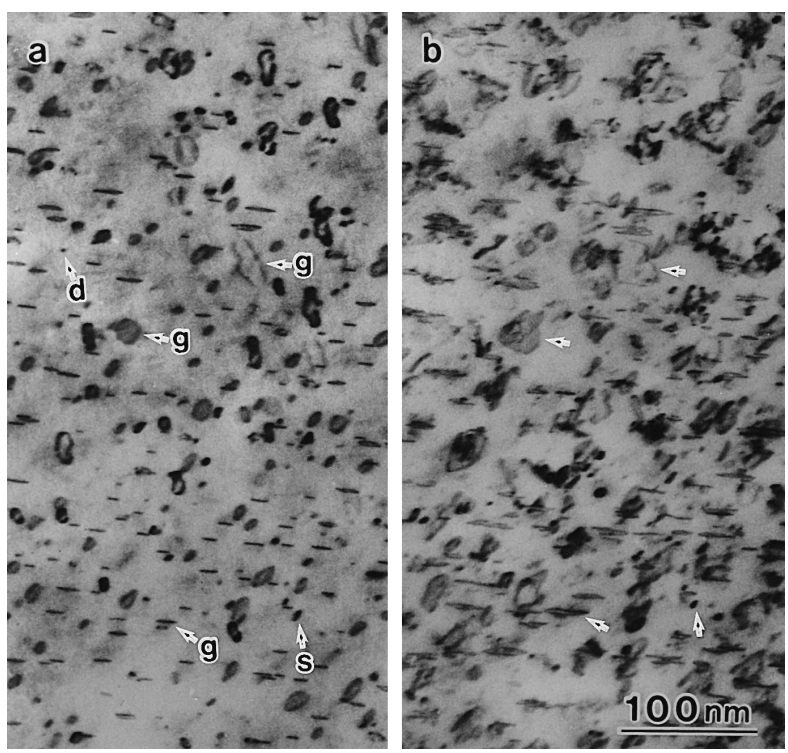

Fig. 5. Comparison of defect structure in a thick part of Fe–16Ni–15Cr neutron irradiated thin foil (1.0×10^{24} n/m^2) at 573 K, between (a) before and (b) after electron irradiation (1000 keV, 4×10^{26} e/m^2) at 573 K.

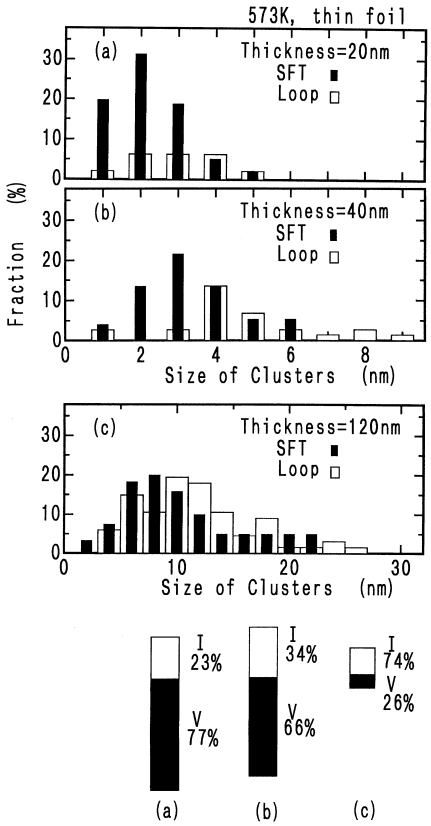

Fig. 6. Size distribution and fraction of I- and V-type defect clusters identified in Fe–16Ni–15Cr neutron irradiated thin foil (1.0×10^{24} n/m^2) at 573 K by electron irradiation at various thickness.

decreases, while the size of both types of defect clusters increases. In more detail, the variation along the depth direction has been examined. Fig. 7 shows the depth distribution of both types of defect clusters identified in the thin and thick part of the specimen foil corresponding to Figs. 1 and 5, respectively. In Fig. 7a, in which the thickness increases from left to right, the fraction of I-type defect clusters is very small in the thinner part, and becomes larger in the thicker part. In the thick part (Fig. 7b), the number density of defect clusters is very low especially at the central part of depth direction.

4.2. Identification of neutron irradiation induced defect clusters in bulk specimens

4.2.1. Behavior of defects introduced by neutron irradiation at a vacancy immobile low temperatures

It might be simpler if electron irradiation is performed at the same temperature as the neutron irradiation. However, at a low temperature where vacancies are immobile, as low as at 353 K, the accumulation of vacancies by electron irradiation leads to the formation of new vacancy clusters and makes the nature identification difficult. Fig. 8 shows an example of microstructure change during electron irradiation at a low temperature of 353 K in a bulk specimen neutron irradiated at 353 K. The growth and the disappearance of clusters were not obvious and the formation of new defect clusters was observed by long term irradiation.

In order to avoid this confusion, the specimen was annealed up to a vacancy mobile high temperature 573 K and then was irradiated with electrons at this temperature.

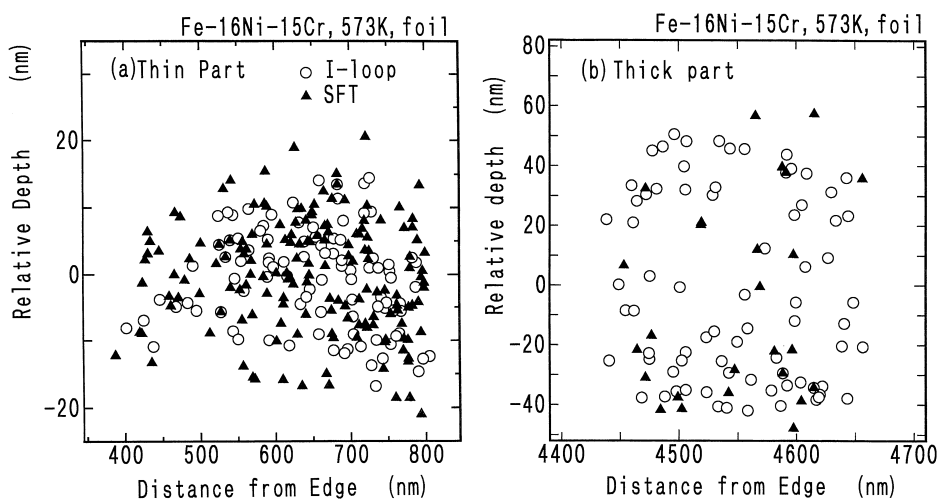

Fig. 7. Cross sectional distribution of defect clusters in a foil specimen shown in Figs. 1 and 5. (a) thin part and (b) thick part. The area for the measurement of the number density in the thick part is 1.45 times wider than in the thin part.

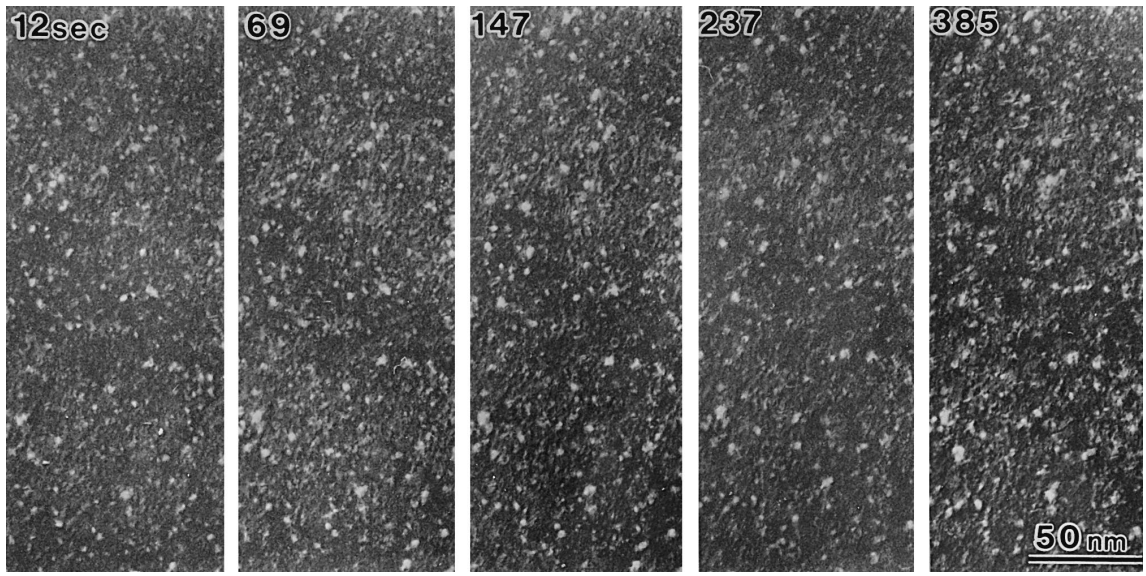

Fig. 8. Progressive change of defect structure in a bulk specimen neutron irradiated (1.1×10^{24} n/m^2) at 353 K during electron irradiation (1000 keV, 2.4×10^{24} e/m^2 s) at 353 K.

Fig. 9a shows a microstructure of the above specimen at the thickness of about 40 nm. I- and V-type clusters may coexist among the fine defect clusters. Fig. 9b shows the same area as Fig. 9a after an isochronal annealing for 30 min by 50 K step up to 573 K. About 40% of defect clusters disappeared by the annealing. Fig. 9c is the microstructure after the electron irradiation following the annealing. Examples of corresponding clusters among three

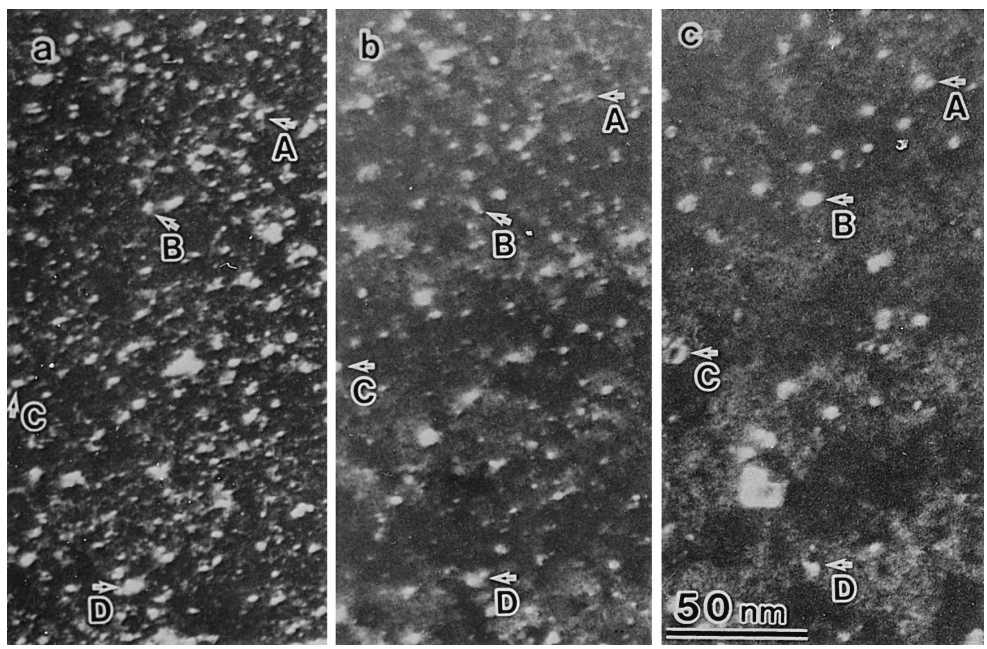

Fig. 9. Defect structures in Fe–16Ni–15Cr neutron irradiated bulk specimen (1.1×10^{24} n/m^2) at 353 K. (a) as irradiated, (b) after an annealing at 573 K for 30 min, (c) after electron irradiation (1000 keV, 1.5×10^{27}e/m^2) at 573 K.

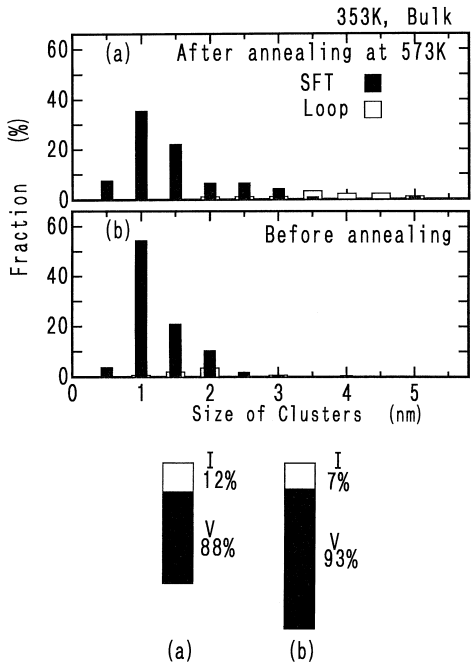

Fig. 10. Size distribution and fraction of I- and V-type clusters in a Fe–16Ni–15Cr neutron irradiated bulk specimen (1.1×10^{24} n/m^2) identified by electron irradiation at 353 K, (a) after the annealing, and (b) before the annealing.

photographs were indicated by the arrows of *A* to *D*. The change from Fig. 9b to Fig. 9c shows that the reactions of defect clusters during electron irradiation proceeded smoothly and that the identification became possible.

Fig. 10a shows the size distribution of I- and V-type defect clusters identified in the annealed specimen. The fraction of I- and V-type defect clusters was 12% and 88%, respectively. The behavior of each defect cluster was traced all through the annealing and electron irradiation, and the image contrast of most of the defect clusters which disappeared in the annealing was found to be similar to that disappeared by the subsequent electron irradiation. Therefore, the defect clusters disappeared by the annealing up to 573 K are assigned to V-type clusters. Fig. 10b shows the original size distribution of defect clusters in as irradiated specimen. Finally, the number densities of I- and V-type defect clusters in the as-irradiated specimen at 353 K were evaluated 3.5×10^{23}/m^3 (7%) and 4.7×10^{24}/m^3 (93%), respectively.

4.2.2. Behavior of defects introduced by neutron irradiation at a vacancy mobile higher temperature

Fig. 11 shows the change of microstructures by the electron irradiation at 573 K in a specimen neutron-irradiated as bulk at 623 K. Most of the defect clusters were well developed dislocation loops, and they naturally grew by

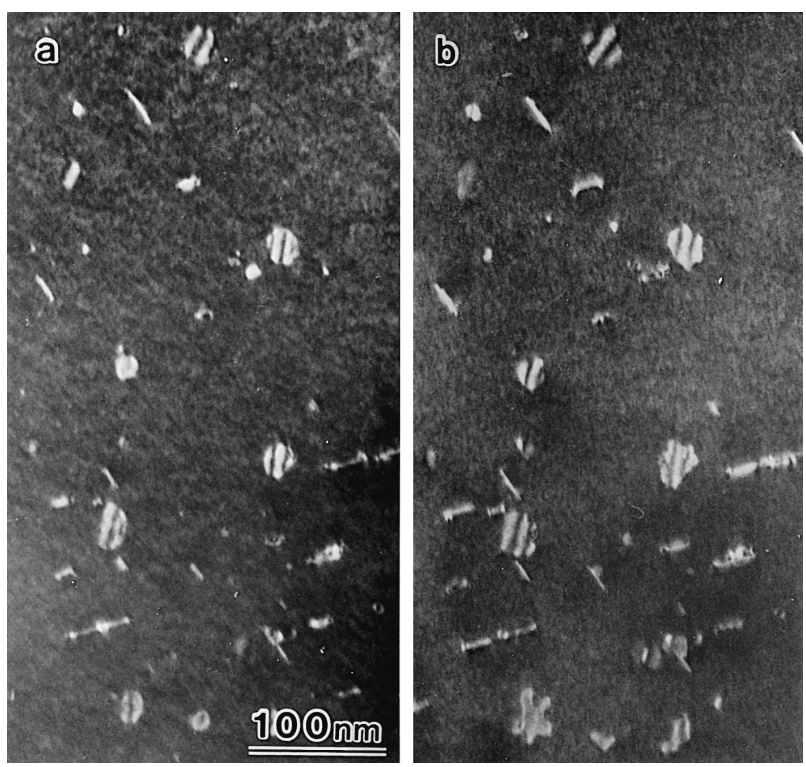

Fig. 11. Comparison of defect structures in a Fe–16Ni–15Cr neutron irradiated bulk specimen (1.1×10^{24} n/m^2) at 623 K, between (a) before and (b) after electron irradiation (1000 keV, 6.5×10^{27} e/m^2) at 573 K.

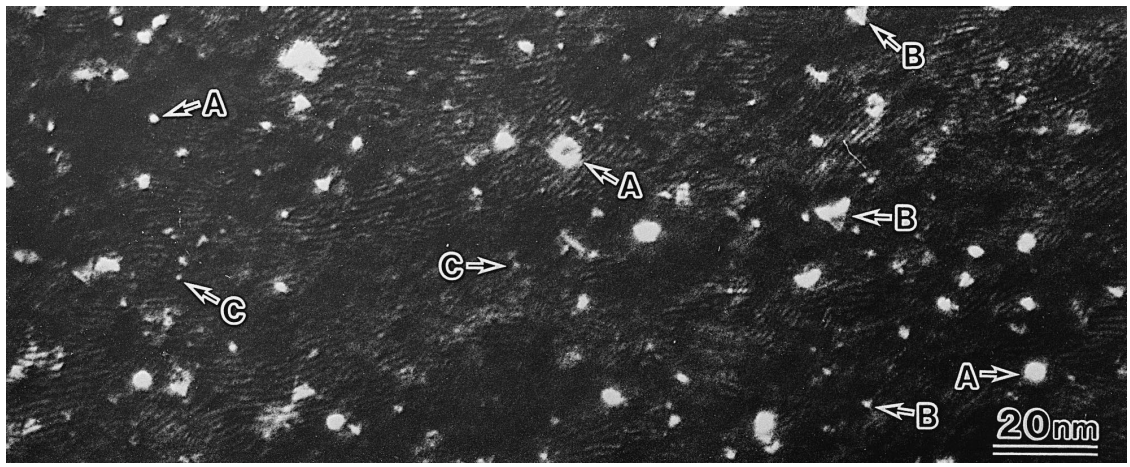

Fig. 12. Microstructure in a Fe–16Ni–15Cr neutron irradiated bulk specimen (1.0×10^{24} n/m^2) at 473 K. Dark-field observation.

electron irradiation showing themselves to be of I-type. Small defects, though very few, disappeared by electron irradiation are thought to be of V-type. The number density of I-type defect clusters was evaluated to be $1.4 \times 10^{21}/\mathrm{m}^3$. The results indicate that V-type defect clusters like SFT, formed directly from collision cascades, become very unstable at 623 K and that almost all vacancies are released from cascade region as freely migrating defects, and contribute to the reaction of point defects: for example, the formation of another V-type defect clusters, namely voids.

4.3. Examination of the pervious judgement of the defect type

In our previous study [1], the judgement of the nature of point defect clusters in Fe–16Ni–15Cr alloy was made only from the shape and contrast of their TEM images. Fig. 12 shows a dark-field TEM image in a specimen neutron irradiated at 473 K as a bulk. The defect clusters are observed along a ⟨110⟩ direction by sing (200) reflection. The deviation from the Bragg condition is $n = 7$.

When the size of defect clusters is more than 2 nm, their nature can be identified from their shape and contrast. The image of I-type clusters has the shape of circle or ellipse. Typical examples are indicated by the arrows of *A*. The image of SFT indicated by the arrows of *B* has the shape of triangle. When the size of clusters becomes smaller than about 2 nm, the identification of the nature is difficult from their shape and contrast. However, almost all these small clusters with the clear image contrast indicated by the arrow of *C* were disappeared by electron irradiation and so they are judged to be of V-type. For Fe–16Ni–15Cr irradiated with neutrons, the judgement that almost all clusters smaller than 1.5 nm are V-type will not be misleading.

Image shape and contrast under bright-field and weak-beam dark-field images which were dealt in Sections 4.1 and 4.2 were the only sources of the judgement. Based on the present study, the authors have confidence that all the defect clusters behave under electron irradiation as expected from the image contrast. These fractions and sizes derived by the previous study agree considerably well with the present results of the bulk specimen irradiated at 353 K [1]. The results of the specimen irradiated at 573 K as a thin foil also agree with each other. In conclusion the judgments by TEM images and those by additional electron irradiation have a good consistency with each other. The comparison of the two types of judgments enhances their confidence.

References

[1] M. Horiki, M. Kiritani, J. Nucl. Mater. 212–215 (1994) 246.
[2] G.W. Groves, A. Kelly, Phil. Mag. 6 (1961) 1527.
[3] D.J. Mazey, R.S. Barnes, A. Howie, Phil. Mag. 7 (1962) 1861.
[4] J.B. Mitchell, W.L. Bell, Acta Metal. 24 (1976) 147.
[5] S. Kojima, Y. Satoh, H. Taoka, I. Ishida, T. Yoshiie, M. Kiritani, Phil. Mag. A 59 (1989) 519.
[6] M. Kiritani, Ultramicroscopy 39 (1991) 135.
[7] M. Kiritani, J. Nucl. Mater. 169 (1989) 89.
[8] A.D. Brailsford, R. Bullough, Phil. Trans. Roy. Soc. 302 (1981) 87.
[9] T. Yoshiie, K. Hamada, S. Kojima and M. Kiritani, Defect and Diffusion Forum 95–98 (1993) 243.
[10] M. Kiritani, T. Yoshiie, S. Kojima, Y. Sotoh, K. Hamada, J. Nucl. Mater. 174 (1990) 327.